Modeling and Force Control for the Collaborative Manipulation of Deformable Strip-Like Materials

authored by **S. Flixeder, T. Glück, and A. Kugi**

and published in *Proceedings of the 7th IFAC Symposium on Mechatronic Systems & 15th Mechatronics Forum International Conference*.

Cite this article as:

S. Flixeder, T. Glück, and A. Kugi, "Modeling and force control for the collaborative manipulation of deformable strip-like materials", in *Proceedings of the 7th ifac symposium on mechatronic systems & 15th mechatronics forum international conference*, Loughborough, UK, Sep. 2016, pp. 95–102. DOI: 10.1016/j.ifacol.2016.10.518

BibTex entry:

```
@INPROCEEDINGS{Flixeder16,
  author = {Flixeder, S. and Gl\"uck, T. and Kugi, A.},
  title = {Modeling and Force Control for the Collaborative Manipulation of
        Deformable Strip-Like Materials},
  booktitle = {Proceedings of the 7th IFAC Symposium on Mechatronic Systems \& 15th
        Mechatronics Forum International Conference},
  year = {2016},
  pages = {95-102},
  address = {Loughborough, UK},
  month = {sep},
  doi = {10.1016/j.ifacol.2016.10.518}
}
```

Link to original paper:

http://dx.doi.org/10.1016/j.ifacol.2016.10.518

Contact:

Automation and Control Institute (ACIN)
TU Wien
Gusshausstrasse 27-29/E376
1040 Vienna, Austria

Internet: www.acin.tuwien.ac.at
E-mail: office@acin.tuwien.ac.at
Phone: +43 1 58801 37601
Fax: +43 1 58801 37699

Modeling and Force Control for the Collaborative Manipulation of Deformable Strip-Like Materials

Stefan Flixeder * **Tobias Glück** * **Andreas Kugi** *

* *Automation and Control Institute (ACIN), TU Wien, 1040 Vienna, Austria (e-mail: {flixeder;glueck;kugi}@acin.tuwien.ac.at)*

Abstract: This work analyzes and evaluates state-of-the-art force control strategies for the collaborative multi-arm handling of deformable materials. We exploit and validate the well-known catenary equation to predict the materials sag and interaction stiffness. The material properties are considered in the manipulator design and coupled system stability is investigated including the dynamics of a first-order force low-pass filter. The analysis provides practical relevant conditions for the selection of the force controller parameters. Different force control strategies are implemented on a multi-arm manipulator, comprising two biaxial gantries, and are evaluated in the light of praxis-oriented case studies.

Keywords: Force Control, Impedance Control, Deformable Materials, Collaborative Handling

1. INTRODUCTION

Deformable materials like textiles, leather, porous tissues, and adhesive foils are used in many industries. Typical manipulation tasks in the cloth, shoe, and garment industry involve transportation, handling, and folding. Similar tasks are encountered in composite manufacturing for the lay-up of preimpregnated or dry fabric sheets on a mold. Although economically important, the manipulation of this material class is hardly automated and hence still labor intensive, time consuming, and lacks of reproducibility, see, e. g., Saadat and Nan (2002) and Lankalapalli and Eischen (2003).

Automatic manipulation of deformable materials is challenging because of their low bending stiffness and geometric diversity. Typical solutions from the field of machine tool engineering focus on the design of highly-sophisticated, special-purpose end-effectors mounted on a single manipulator, e. g., area- or multi-gripper, see Fig. 1. The approach, however, is rather inflexible and becomes inefficient for large-scale objects or more complex tasks, e. g., folding or lay-up on non-flat surfaces. Recently, several authors proposed a more human-like approach, namely, the cooperation of multiple manipulators. For example, the multi-functional cell of Krebs et al. (2013) consists of two industrial robots mounted on gantries. The handling and the lay-up of a preimpregnated composite sheet is based on pure position control. Koustoumpardis and Aspragathos (2008) present a robot manipulator collaborating with a human to handle a fabric based on a neural network force controller. Besides force feedback, the follow-up work of Koustoumpardis et al. (2016) additionally exploits visual feedback to percept the humans intention. Their robot manipulator is capable of folding a rectangular piece of fabric by human guidance. An approach to collaboratively manipulate a deformable sheet between a person and a dual-armed robot is presented by Kruse et al. (2015). To follow the human motion, the robot utilizes a hybrid controller which combines force and vision information. A comprehensive review on the challenges and solutions on the robotic manipulation of deformable objects is provided by Khalil and Payeur (2010). During the handling of deformable materials it is crucial to maintain the appropriate amount of internal tension force, i. e., a tension force which is high enough to avoid sagging or wrinkles and low enough to avoid tearing or loss of gripping. To solve the force controlled manipulation problem, different control strategies are presented in literature, see, e. g., Zeng and Hemami (1997); De Schutter et al. (1998); Vukobratovic et al. (2009). These strategies, however, have hardly been applied to the coordinated manipulation of deformable materials. One reason is the complex interaction behavior between the manipulator and the handling object during physical contact.

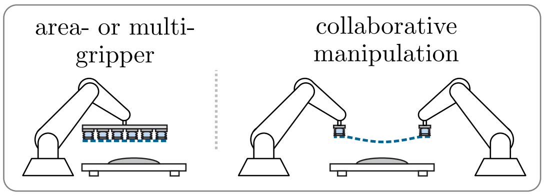

Fig. 1. Different approaches for the manipulation of deformable materials.

Although a number of mathematical models for the shape prediction of this material class are available, see, e. g., Henrich and Wörn (2000); Syerko et al. (2012), they are hardly used for control, mainly due to their complexity. A rather simple, but interesting modeling approach proposed by Grießer and Taylor (1996) is based on potential and bending energy stored in a two-edges lifted fabric. A closer examination of their work reveals that the derived ana-

⋆ This work was supported by Festo AG & Co. KG

Post-print version of the article: S. Flixeder, T. Glück, and A. Kugi, "Modeling and force control for the collaborative manipulation of deformable strip-like materials", in *Proceedings of the 7th ifac symposium on mechatronic systems & 15th mechatronics forum international conference*, Loughborough, UK, Sep. 2016, pp. 95–102. doi: 10.1016/j.ifacol.2016.10.518
The content of this post-print version is identical to the published paper but without the publisher's final layout or copy editing.

lytical function is equivalent to the well-known catenary equation, see, e. g., Routh (1891).

In order to enable and support the coordination of multiple manipulators for the handling of deformable materials, this work exploits and validates the catenary equation as a suitable interaction model for strip-like objects. Utilizing parallel position and force control, which generalizes pure force and impedance control, and a low-pass force filter in the loop, an extension of the coupled system stability criterion proposed by Šurdilović (2007) will be presented. The stability analysis provides practically relevant conditions for the selection of the controller parameters and motivates an intrinsic compliance in the mechatronic manipulator design to further enhance the force control performance. Moreover, different force control implementations on a multi-arm manipulation system are experimentally evaluated and compared in view of a collaborative handling approach.

The paper is organized as follows: Section 2 utilizes the catenary model to determine the materials shape and interaction parameters. Moreover, an appropriate model of the considered multi-arm manipulation system consisting of two biaxial gantry robots is introduced. Section 3 briefly classifies state-of-the-art force control strategies and provides a stability analysis for the general parallel position and force control approach with additional force low-pass filtering in the loop. Finally, Section 4 presents experimental results and compares different force controller implementations for the collaborative handling of a deformable strip-like material. In a future work, the results of this publication will be utilized for a collaborative layup of deformable materials on a complex mold.

2. MATHEMATICAL MODELING

The following section introduces suitable mathematical models for the deformable material to be handled and the multi-arm manipulation system. These models serve for simulation purposes and model based controller design.

2.1 Deformable Material

While most modeling approaches are essentially developed for material design and the prediction of tensile and bending properties, only a few models allow for real-time shape prediction. As previously mentioned, the model of Grießer and Taylor (1996) for a strip-like fabric leads to the well-known catenary equation. Subsequently, this static equation is used to predict the shape and the stiffness of a two-edges lifted, strip-like, deformable material.

A catenary is a curve of an idealized hanging string under its own weight, see Fig. 2. With regards to strip-like, deformable materials it is assumed that the material is so thin that any tension force exerted by the string is tangential to the string (zero bending stiffness). Moreover, the mass per unit length is considered uniform and does not change with tension. Let us consider the schematic of a catenary hanging between two supporting points GA_i, with $i \in \{1, 2\}$, as depicted in Fig. 2. Since only gravitational forces act along the negative z-axis, the y-component of the force is uniform at each point of the string and $F_y = F_{\mathrm{GA}_1,y} = F_{\mathrm{GA}_2,y}$ holds. Utilizing calculus

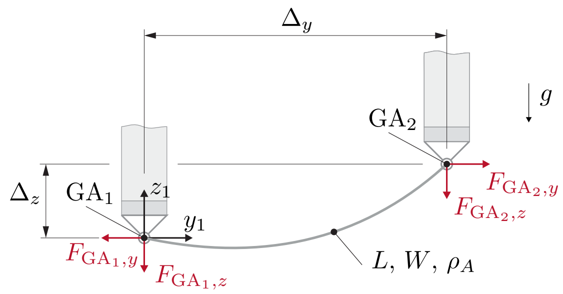

Fig. 2. Catenary with length L, width W, and area density ρ_A under its own weight supported at the grasping points GA_i, $i \in \{1, 2\}$.

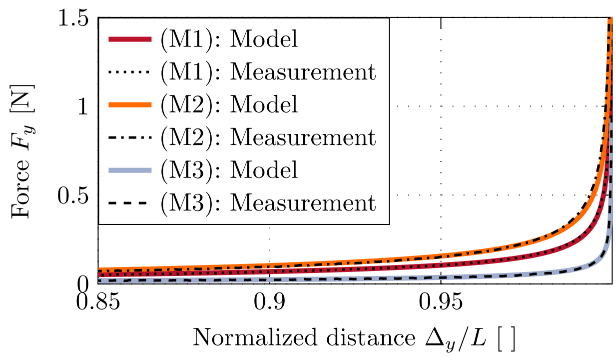

Fig. 3. Horizontal force F_y subject to a normalized distance variation Δ_y/L for various materials, see Table 1.

of variations, the catenary equation reads as, see, e. g., Routh (1891),

$$z = \frac{F_y}{q}\cosh\left(\frac{q}{F_y}y + C_1\right) + C_2 \ , \tag{1}$$

with $q = g\rho_A W$, where g denotes the gravitational acceleration $g = 9.81\,\mathrm{m\,s^{-2}}$, ρ_A is the area density, and W is referred to as the catenary width. The parameters C_1, C_2, and F_y depend on the boundary conditions. Evaluation of (1) with respect to the boundary conditions at the supporting points $z|_{y=0} = 0$ and $z|_{y=\Delta_y} = \Delta_z$ in combination with the catenary length

$$L = \int_0^{\Delta_y} \sqrt{1 + \left(\frac{\mathrm{d}z}{\mathrm{d}y}\right)^2}\,\mathrm{d}y \tag{2}$$

yields the transcendental equation

$$\left(2\frac{F_y}{q}\sinh\left(\frac{q}{2F_y}\Delta_y\right)\right)^2 + \Delta_z^2 - L^2 = 0 \ , \tag{3}$$

with one unknown parameter F_y. Equation (3) can be solved numerically using, e. g., Newton's method, and has at most one solution with $F_y > 0$. The integration constants C_1 and C_2 are derived by means of the remaining independent equations

$$C_1 = \operatorname{atanh}\left(\frac{\Delta_z}{L}\right) - \frac{q\Delta_y}{2F_y} \ , \quad C_2 = -\frac{F_y \cosh C_1}{q} \ . \tag{4}$$

Fig. 3 shows the modeled and measured horizontal force F_y subject to a distance variation Δ_y of the supporting points for a constant distance $\Delta_z = 0$ and different strip-like materials listed in Table 1. Note that although the static model solely relies on the material parameters L, W, and ρ_A, the model (1) fits the measurements very well. The

Post-print version of the article: S. Flixeder, T. Glück, and A. Kugi, "Modeling and force control for the collaborative manipulation of deformable strip-like materials", in *Proceedings of the 7th ifac symposium on mechatronic systems & 15th mechatronics forum international conference*, Loughborough, UK, Sep. 2016, pp. 95–102. DOI: 10.1016/j.ifacol.2016.10.518
The content of this post-print version is identical to the published paper but without the publisher's final layout or copy editing.

Table 1. Technical characteristics of the considered fiber materials. ID = identifier, NC = non-crimp, UD = uni-directional

ID	description	width W [mm]	area density ρ_A [g m^{-2}]	length L [mm]
(M1)	glas, plain weave	80	225	700
(M2)	carbon, NC, UD	75	250	1000
(M3)	adhesive tape	38	115	1000

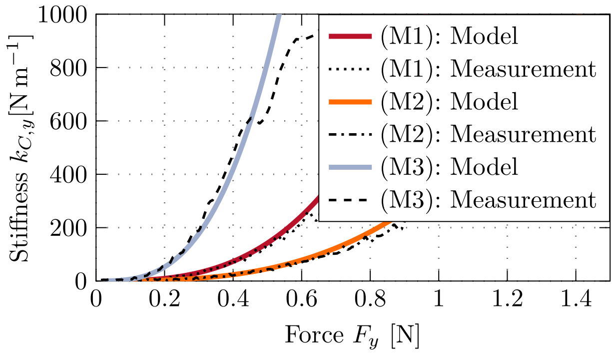

Fig. 4. Measured and modeled catenary stiffness $k_{C,y}$ of a strip-like material subject to a horizontal force F_y.

experiment demonstrates that the considered materials comply with the assumptions of an ideal catenary, i. e., low bending stiffness and high tension stiffness.

Obviously, the relationship between distance and force is highly nonlinear, in particular for the case of a normalized distance Δ_y/L close to one, see Fig. 3. The gradient of the curve can be interpreted as the horizontal tension stiffness $k_{C,y}$ opposed by material for a given set-point Δ_y. To determine $k_{C,y}$, the first partial derivative of (3) with respect to Δ_y is calculated in the form

$$\frac{-4q\Delta_y \sinh\left(\frac{q\Delta_y}{2F_y}\right)\cosh\left(\frac{q\Delta_y}{2F_y}\right) + 8F_y \sinh\left(\frac{q\Delta_y}{2F_y}\right)^2}{q^2} k_{C,y} + \frac{4F_y \sinh\left(\frac{q\Delta_y}{2F_y}\right)\cosh\left(\frac{q\Delta_y}{2F_y}\right)}{q} = 0 \ . \tag{5}$$

Finally, the catenary stiffness $k_{C,y}$ can be directly obtained from (5) for a given set of measurements Δ_y and F_y.

Fig. 4 compares the stiffness obtained from measurement data using numerical differentiation and the stiffness model (5). Apparently, the model agrees well with the measured stiffness, although, it solely relies on the nominal parameters W and ρ_A as well as the measurements of Δ_y and F_y. In view of the intended force based handling strategy, the considerable increase of the stiffness $k_{C,y}$ for higher forces F_y potentially causes stability problems in force control, see Section 3.2. As will be shown in the course of this work, these stability problems can be circumvented by an appropriate mechatronic design, i. e., an intrinsic compliance of the manipulator's end-effector.

2.2 Multi-Arm Manipulator

The considered multi-arm manipulator comprises of two grasping arms $k \in \{\mathrm{GA}_1, \mathrm{GA}_2\}$, each consisting of a two-dimensional (2-DOF) gantry and an end-effector, see

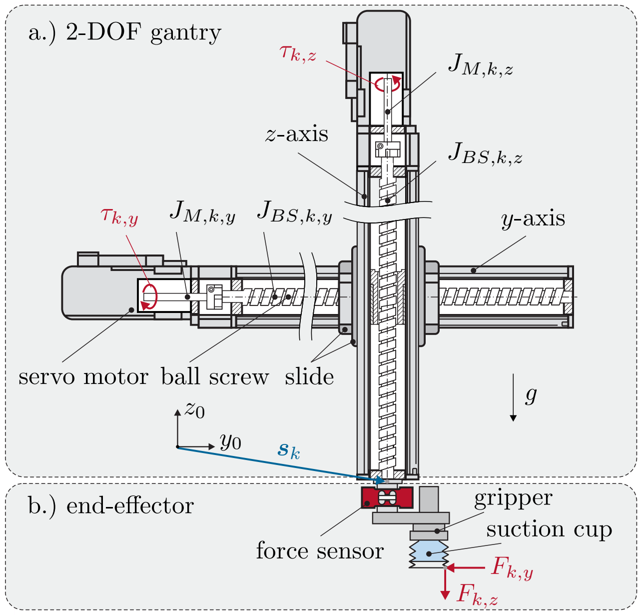

Fig. 5. Schematic diagram of a grasping arm, with $k \in \{\mathrm{GA}_1, \mathrm{GA}_2\}$.

Table 2. Components of a grasping arm.

component	manufacturer	type
y-axis ball screw	Festo	*EGC-80-BS-KF-600*
z-axis ball screw	Festo	*EGC-70-BS-KF-800*
servo motor	Festo	*AS-55-M*
force sensor	ME-Messsysteme	*K3D40*

Table 3. Parameters of the 2-DOF gantry.

j-axis	$m_{T,k,j}$	$m_{J,k,j}$	$F_{c,k,j}$	$c_{v,k,j}$
y-axis	12.77 kg	21.37 kg	47.3 N	238.8 N s m^{-1}
z-axis	8.93 kg	17.62 kg	54.5 N	187.8 N s m^{-1}

Fig. 5. The end-effectors are equipped with force sensors, grippers, and compliant suction cups.

A dynamic model of a 2-DOF gantry of a similar setup was introduced in Flixeder et al. (2014) and is briefly revisited in the following. As depicted in Fig. 5a.), $\mathbf{s}_k^{\mathrm{T}} = [s_{k,y} \ s_{k,z}]$ refers to the position of the end-effector with respect to the reference frame (y_0, z_0). Moreover, $m_{T,k,j}$ denotes the moved mass (including the end-effector mass) of each axis, $p_{k,j}$ the spindle pitch, and $m_{J,k,j} = (J_{M,k,j} + J_{BS,k,j})/p_{k,j}^2$ the equivalent mass of the inertia of the servo drive $J_{M,k,j}$ and the ball screw $J_{BS,k,j}$, respectively. The actual motor torques $\tau_{k,j}$, $j \in \{y, z\}$ serve as control inputs to the system because of the fast subordinate current controllers. The equivalent motor force reads as $F_{M,k,j} = \tau_{k,j}/p_{k,j}$ and the load force on the end-effector is denoted by $F_{k,j}$. Furthermore, the friction force of the ball screw drives is modeled as $F_{F,k,j} = \tanh(\dot{s}_{k,j}/w)F_{c,k,j} + c_{v,k,j}\dot{s}_{k,j}$, with $w \ll 1$, and the viscous and Coulomb friction coefficients $c_{v,k,j} > 0$ and $F_{c,k,j} > 0$. Details on the different components of the grasping arms are listed in Table 2. The model parameters provided in Table 3 are either extracted from data sheets or measurements.

Post-print version of the article: S. Flixeder, T. Glück, and A. Kugi, "Modeling and force control for the collaborative manipulation of deformable strip-like materials", in *Proceedings of the 7th ifac symposium on mechatronic systems & 15th mechatronics forum international conference*, Loughborough, UK, Sep. 2016, pp. 95–102. doi: 10.1016/j.ifacol.2016.10.518

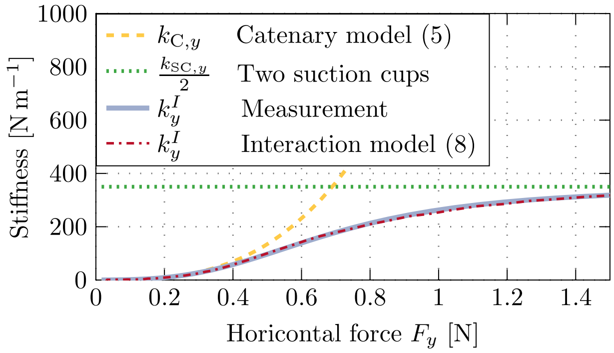

Fig. 6. Measured and modeled interaction stiffness k_y^I as a function of F_y for fabric (M2) and length $L = 0.7\,\mathrm{m}$.

Because of the high mechanical rigidity and the sturdy construction, the coupling between the motor, the ball screw drives, and the mechanic connection between the two axis are assumed stiff and backlash-free. Hence, the axis dynamics are decoupled and the equations of motion for each axis $j \in \{y, z\}$ read as

$$\ddot{s}_{k,j} = f_{k,j} + G_{k,j} F_{M,k,j} - G_{k,j} F_{k,j} \ , \tag{6}$$

with

$$f_{k,y} = \frac{-F_{F,k,y}(\dot{s}_{k,y})}{m_{T,k,y} + m_{J,k,y}} \ , \qquad G_{k,y} = \frac{1}{m_{T,k,y} + m_{J,k,y}} \ ,$$
$$f_{k,z} = \frac{-F_{F,k,z}(\dot{s}_{k,z}) - g m_{T,k,z}}{m_{T,k,z} + m_{J,k,z}} \ , \quad G_{k,z} = \frac{1}{m_{T,k,z} + m_{J,k,z}} \ . \tag{7}$$

For the subsequent controller design, the end-effector dynamics are neglected, because the eigenfrequencies of the force sensors and suction cups are a magnitude higher than the target dynamics typically observed in human arm operation and active compliance control. The stiffness of the suction cup, $k_{SC,y} = 700\,\mathrm{N\,m^{-1}}$, was experimentally determined as the mean value of the stiffness in the force range $F_y = 0$ - $1.5\,\mathrm{N}$. The rather low stiffness will be considered by an interaction model.

2.3 Interaction Model

The interaction model characterizes the physical connection between the grasping arms. For the controller design this connection is typically modeled as a most destabilizing environment of a pure spring element, see Colgate and Hogan (1988). For the considered multi-arm configuration, the horizontal interaction stiffness sums up as a series connection of three spring elements, i. e., two suction cups and the handling material. Thus, the interaction model reads as

$$k_y^I = \frac{k_{C,y} \frac{k_{SC,y}}{2}}{k_{C,y} + \frac{k_{SC,y}}{2}} \ , \tag{8}$$

with the catenary tension stiffness $k_{C,y}$ according to (5) and the stiffness of the suction cup $k_{SC,y}$. As shown in Fig. 6, the model (8) agrees well with the measured stiffness k_y^I.

Note that k_y^I, though a function of the force F_y, is bounded by the intrinsic compliance of the suction cup with $0 < k_y^I < \frac{k_{SC,y}}{2}$. The implication of this upper bound on the interaction stiffness is discussed in the course of the next section.

3. CONTROL METHODS

The controller design is based on the models presented in Section 2. Available measurements are the external load force $\boldsymbol{F}_k^\mathrm{T} = [F_{k,y}\ F_{k,z}]$ as well as the position $\boldsymbol{s}_k^\mathrm{T} = [s_{k,y}\ s_{k,z}]$, and velocity $\dot{\boldsymbol{s}}_k^\mathrm{T} = [\dot{s}_{k,y}\ \dot{s}_{k,z}]$ of the handling arms calculated from the measurements of the integrated motor encoders. For the ease of notation, the index denoting the grasping arm $k \in \{\mathrm{GA}_1, \mathrm{GA}_2\}$ and the direction $j \in \{y, z\}$ are suppressed in the following. To solve the collaborative manipulation problem several control strategies are employed.

3.1 Position Control

Feedback linearization, see, e. g., Isidori (1995), is used for position control. The first- and second-order time-derivative of the position output $y = s$ reads as (see (6))

$$\dot{y} = \dot{s} \ , \quad \ddot{y} = f + G F_M - G F \ . \tag{9}$$

Introducing the new input $\tilde{u} = \ddot{y}$ and solving (9) for the motor force F_M yields the feedback transformation

$$F_M = \frac{1}{G}(-f + \tilde{u}) + F \ . \tag{10}$$

The controller

$$\tilde{u} = \ddot{s}^p - a_2 \dot{e}_s^p - a_1 e_s^p - \int_0^t a_0 e_s^p \mathrm{d}\tau \tag{11}$$

with position error $e_s^p = s - s^p$ and sufficiently smooth reference s^p yields an exponentially stable error dynamics that can be arbitrarily assigned by suitable constants a_i, $i = 0, 1, 2$. An anti-windup strategy is used to account for input constraints.

3.2 Force Control

For a comprehensive literature overview on robotic force control, see, e. g., Zeng and Hemami (1997); De Schutter et al. (1998); Vukobratovic et al. (2009). Basically, two groups of robotic force control strategies are distinguished, i. e. pure force control and impedance control. Force control aims at following a prescribed force reference. In practice, however, force measurement is typically corrupted by noise and hence damping is difficult to implement, see, e. g., Wedel and Saridis (1988). By contrast, the idea of impedance control is to establish a desired relationship between effort and motion.

A combination of the two approaches is the so called parallel position and force control (PPFC) strategy, see Chiaverini et al. (1992). Typically, the target dynamics of PPFC are specified in the form

$$e_F + a_0^F \int_0^t e_F \mathrm{d}\tau = m^d \ddot{e}_s + d^d \dot{e}_s + k^d e_s \ , \tag{12}$$

with force error $e_F = F - F^d$ and position error $e_s = s - s^d$, where s^d and F^d denote the reference position and force, respectively. The constant parameters m^d, d^d, and k^d represent the desired inertia, damping, and stiffness of the target dynamics. The constant parameter a_0^F refers to the integration coefficient of the force error. Note that pure force control and impedance control are special cases of PPFC. Pure force control is obtained by setting $d^d = k^d = 0$ in (12) and the target dynamics of impedance control are equivalent to (12) for $a_0^F = F^d = 0$.

Post-print version of the article: S. Flixeder, T. Glück, and A. Kugi, "Modeling and force control for the collaborative manipulation of deformable strip-like materials", in *Proceedings of the 7th ifac symposium on mechatronic systems & 15th mechatronics forum international conference*, Loughborough, UK, Sep. 2016, pp. 95–102. DOI: 10.1016/j.ifacol.2016.10.518
The content of this post-print version is identical to the published paper but without the publisher's final layout or copy editing.

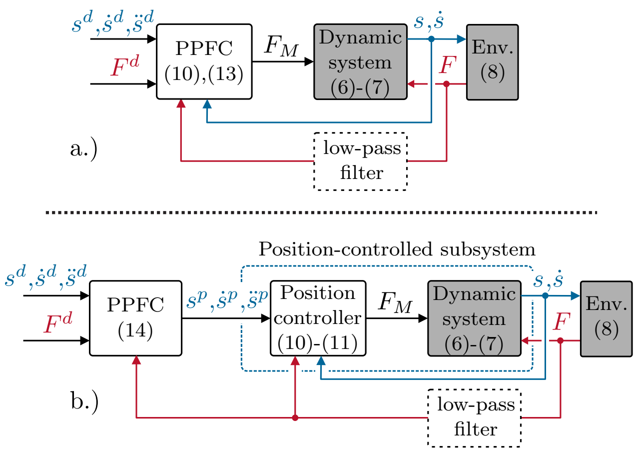

Fig. 7. Different implementations of parallel position and force control (PPFC): a.) explicit, b.) implicit.

With regard to an implementation, a further distinction between explicit (*force-based* or *dynamic-based*) and implicit (*position-based* or *inner/outer*) methods is made, see Fig. 7. The explicit approach utilizes the control law

$$\tilde{u} = \underbrace{\frac{-d^d \dot{e}_s^d - k^d e_s^d}{m^d}}_{\text{position controller}} + \ddot{s}^d + \underbrace{\frac{e_F + a_0^F \int_0^t e_F \mathrm{d}\tau}{m^d}}_{\text{force controller}} \tag{13}$$

in combination with the feedback transformation (10). In contrast, the implicit approach employs an inner loop position controller (10)-(11) to track the reference s^p generated by the outer loop controller. To realize the closed-loop target dynamics (12), the outer control law reads as

$$\ddot{s}^p = \underbrace{\frac{-d^d \dot{e}_s^{pd} - k^d e_s^{pd}}{m^d}}_{\text{position controller}} + \ddot{s}^d + \underbrace{\frac{e_F + a_0^F \int_0^t e_F \mathrm{d}\tau}{m^d}}_{\text{force controller}}$$
$$\dot{s}^p = \int_0^t \ddot{s}^p \mathrm{d}\tau \ , \quad s^p = \int_0^t \dot{s}^p \mathrm{d}\tau \ , \tag{14}$$

with $e_s^{pd} = s^p - s^d$. This implementation allows to account for velocity and acceleration limits of the physical system by conditional execution and integration.

The stability properties of force control strategies are widely discussed in literature, see Zeng and Hemami (1997); Vukobratovic et al. (2009). For simplicity reasons, a perfect feedback compensation of the system dynamics for the explicit implementation and/or a perfect tracking of the inner position loop for the implicit implementation is assumed. Furthermore, let us consider a most destabilizing environment of a pure spring element, see Colgate and Hogan (1988), with the stiffness $k^E > 0$. Hence, a necessary and sufficient condition to ensure stability of (12) is that the target parameters are positive real, see Vukobratovic et al. (2009). However, in practical implementations, the measured force F contains high frequency components due to non-modeled dynamics that, e. g., stem from the force sensor dynamics, the mechanical frame vibrations, and the non-rigid axes coupling. These high frequency components of the measured force signal are typically reduced by low-pass filtering, see Fig. 7. Consequently, the positive realness of the target parameters is no longer sufficient to provide stability of the coupled system.

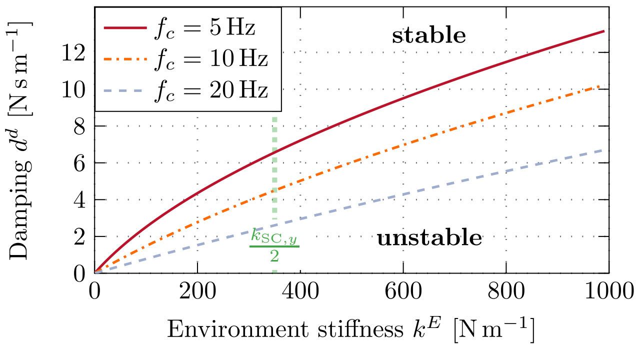

Fig. 8. Stability boundary for different low-pass filter frequencies f_c, $m^d = 0.4$ kg, and $a_0^F = 0$.

The coupled system stability (Šurdilović, 2007, Definition 1) ensures stable interaction between a robotic manipulator under impedance control and a passive environment. Subsequently, we present an extension for the more general case of PPFC with additional low-pass force filtering. Along the lines of Šurdilović (2007), coupled stability is guaranteed, if the transfer function

$$\left[1 + G_d^{-1}(p) G_{\mathrm{PT1}}(p) k^E\right]^{-1} \tag{15}$$

is stable. In (15), $G_d(p) = e_F/e_s$ denotes the target dynamics of (12), k^E corresponds to the environment transfer function, $G_{\mathrm{PT1}}(p)$ refers to a first-order low-pass filter (PT1) with cutoff frequency $f_c = 1/(2\pi T_c)$, and p is the Laplace variable. Following the Routh-Hurwitz stability criterion, the transfer function (15) is stable as long as

$$\begin{aligned}
0 <& d^d + k^d T_c, \quad 0 < m^d + d^d T_c, \\
0 <& a_0^F k^E, \qquad 0 < k^E + k^d, \qquad 0 < m^d T_c, \\
0 <& \left(k^E + k^d\right)\left(d^d + k^d T_c\right) - a_0^F k^E \left(m^d + d^d T_c\right), \\
0 <& \left(k^E + k^d\right)\left(d^d + k^d T_c\right)\left(m^d + d^d T_c\right) \\
& - a_0^F k^E \left(m^d + d^d T_c\right)^2 - m^d T_c \left(k^E + k^d\right)^2
\end{aligned} \tag{16}$$

holds. For given parameters $m^d > 0$, $k^E > 0$, $T_c > 0$, and $k^d = 0$, the lower bound for the damping parameter to ensure stability in terms of (16) computes as

$$d^d > \frac{a_0^F m^d}{1 - a_0^F T_c} \tag{17}$$

and

$$d^d > \frac{\pm\sqrt{m^d\left(m^d + 4k^E T_c^2 - 4a_0^F k^E T_c^3\right)} - m^d\left(1 - 2a_0^F T_c\right)}{2T_c\left(1 - a_0^F T_c\right)} \ . \tag{18}$$

Condition (18) proves to be more restrictive.

Fig. 8 depicts the stability boundary (18) as a function of the environment stiffness k^E and different cutoff frequencies f_c for a desired mass of $m^d = 0.4$ kg and a force error integration coefficient $a_0^F = 0$. Clearly, the stiffer the environment, the more damping is required in order to preserve a stable contact without oscillations. If the damping parameter is chosen higher than actually needed, high transient forces may occur (in the case of an external disturbance) due to the slow target dynamics. Consequently, a proper selection of the damping parameter is essential in order to preserve stability, but also to enable high force control performance. Furthermore, Fig. 8

Post-print version of the article: S. Flixeder, T. Glück, and A. Kugi, “Modeling and force control for the collaborative manipulation of deformable strip-like materials”, in *Proceedings of the 7th ifac symposium on mechatronic systems & 15th mechatronics forum international conference*, Loughborough, UK, Sep. 2016, pp. 95–102. doi: 10.1016/j.ifacol.2016.10.518
The content of this post-print version is identical to the published paper but without the publisher’s final layout or copy editing.

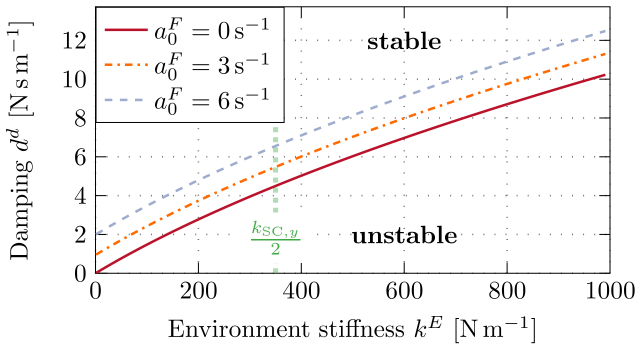

Fig. 9. Stability boundary for various force integration constants a_0^F, a cutoff frequency $f_c = 10\,\mathrm{Hz}$ and a desired mass of $m^d = 0.4\,\mathrm{kg}$.

reveals that the lower the cutoff frequency of the low-pass filter is chosen, the more damping is required in order to preserve stability. Likewise, the increase of the integration coefficient of the force error a_0^F rises the required minimum damping, see Fig. 9.

Note that the concept of coupled system stability is also valid for multiple manipulators handling one object, see Šurdilović et al. (2010). The assumption of a constant environment stiffness $k^E = k_y^I$, however, only holds for a constant force F_y, see (5) and (8). Thus, in view of a varying interaction stiffness k_y^I, condition (18) provides only a local stability criteria. The intrinsic compliance is bounded by $0 < k_y^I < k_{\mathrm{SC}}/2$. Hence, for the subsequent controller tuning, the environment is modeled by a most destabilizing environment element with stiffness $k_{\mathrm{SC}}/2$. Apparently, the target damping d^d can be reduced by a proper mechatronic design of the intrinsic compliance to considerably enhance the force control performance, cf. Fig. 8 and 9.

4. EXPERIMENTAL RESULTS AND DISCUSSION

This section provides experimental results in order to answer the following questions:

- Which one of the two strategies - explicit or implicit force control - is more favorable for the coordinated force control of strip-like deformable materials?
- To what extent does the additional integral term a_0^F of the force error in (12) improve the force tracking performance?

To this end, two simple experiments are designed, see Fig. 10 and 11. For reasons of simplicity, only the y-axis of the grasping arm (GA_1) is force controlled, while the z-axis of (GA_1) as well as both axes of (GA_2) are position controlled. The desired stiffness $k^d_{\mathrm{GA}_1,y}$ of the force controller is set to zero. Thus, the natural frequency of the coupled impedance model reads as $f_{0,\mathrm{GA}_1,y} = \frac{1}{2\pi}\sqrt{k_y^I/m^d_{\mathrm{GA}_1,y}}$. A desired mass of $m^d_{\mathrm{GA}_1,y} = 0.4\,\mathrm{kg}$ ensures that $f_{0,\mathrm{GA}_1,y}$ is well below the mechanical resonance frequency $f_{0,\mathrm{mech}} \approx 11\,\mathrm{Hz}$. In order to guarantee coupled system stability, the target damping $d^d_{\mathrm{GA}_1,y}$ is chosen 50 % higher than the minimum damping $d^{\min}_{\mathrm{GA}_1,y}$ required by the stability criterion (18). The cutoff frequency of the PT1 force filter is set to $f_c = 10\,\mathrm{Hz}$. The parameters $a_{i,j,k}$, with $i = \{0,1,2\}$, $k \in \{\mathrm{GA}_1, \mathrm{GA}_2\}$ and $j \in \{y,z\}$ of the position controller are chosen so that the eigenvalues of the closed-loop error dynamics are $p_{i,j,k} = -70\,\mathrm{s}^{-1}$.

Fig. 10. Exp. 1: The position controlled grasping arm (GA_2) moves in a circular trajectory while the force controlled one (GA_1) maintains a constant tension force by adjusting its horizontal position.

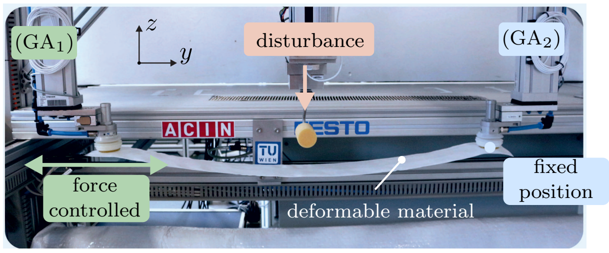

Fig. 11. Exp. 2: An external disturbance penetrates the deformable material. To maintain a constant tension force, the force controlled grasping arm (GA_1) compensates the disturbance by adjusting its y-position.

Table 4. Evaluated implementations of PPFC.

ID	implementation	$a^F_{0,\mathrm{GA}_1,y}$	$d^{\min}_{\mathrm{GA}_1,y}$	$d^d_{\mathrm{GA}_1,y}$
(C1)	explicit	$3\,\mathrm{s}^{-1}$	$6\,\mathrm{N\,s\,m}^{-1}$	$9\,\mathrm{N\,s\,m}^{-1}$
(C2)	implicit	$0\,\mathrm{s}^{-1}$	$4.7\,\mathrm{N\,s\,m}^{-1}$	$7\,\mathrm{N\,s\,m}^{-1}$
(C3)	implicit	$3\,\mathrm{s}^{-1}$	$6\,\mathrm{N\,s\,m}^{-1}$	$9\,\mathrm{N\,s\,m}^{-1}$

All experiments were performed with Material (M1), see Table 1. The considered force controllers are summarized in Table 4 and are implemented and executed using the real-time system DS1006 from dSPACE with a sampling time of 1 ms. The results are presented by means of measurements and a video [1] .

4.1 Experiment 1: Collaborative Handling

The idea of the experiment is to evaluate the properties and suitability of different force control strategies for a coordinated transportation process. In the following scenario, the position controlled grasping arm (GA_2) moves along a circular trajectory with the radius $R = 0.1\,\mathrm{m}$ and the angular velocities of $\omega = 45\,{}^\circ\,\mathrm{s}^{-1}$ and $\omega = 90\,{}^\circ\,\mathrm{s}^{-1}$ in phase ① and ②, respectively. Concurrently, the force controlled grasping arm (GA_1) adjusts its y-position to maintain a desired tension force of $F^d_{\mathrm{GA}_1,y} = 0.35\,\mathrm{N}$. Note that by controlling the horizontal tension force $F_{\mathrm{GA}_1,y}$ the sag of the deformable material is implicitly determined.

The coordination of the two grasping arms is supported by means of the velocity feedforward $\dot{s}^d_{\mathrm{GA}_1,y} = \dot{s}^d_{\mathrm{GA}_2,y}$. Nevertheless, since the vertical movement of (GA_2) is unknown

[1] www.acin.tuwien.ac.at/fileadmin/cds/videos/collabForceCtrl.mp4

Post-print version of the article: S. Flixeder, T. Glück, and A. Kugi, "Modeling and force control for the collaborative manipulation of deformable strip-like materials", in *Proceedings of the 7th ifac symposium on mechatronic systems & 15th mechatronics forum international conference*, Loughborough, UK, Sep. 2016, pp. 95–102. doi: 10.1016/j.ifacol.2016.10.518
The content of this post-print version is identical to the published paper but without the publisher's final layout or copy editing.

ACIN

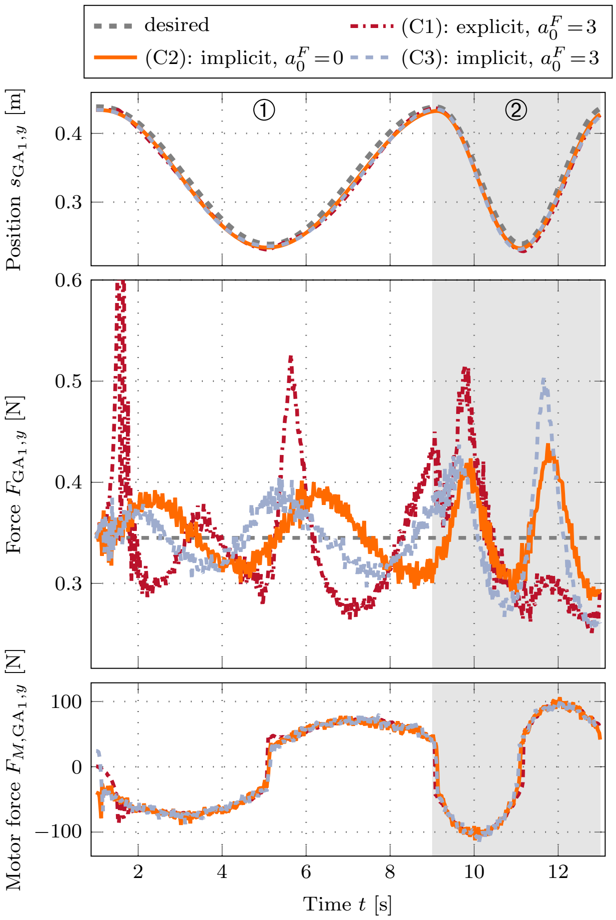

Fig. 12. Exp. 1: (GA_2) moves in a circle while (GA_1) is force controlled and adjusts its y-position to constantly maintain a desired tension force $F^d_{\mathrm{GA}_1,y}$.

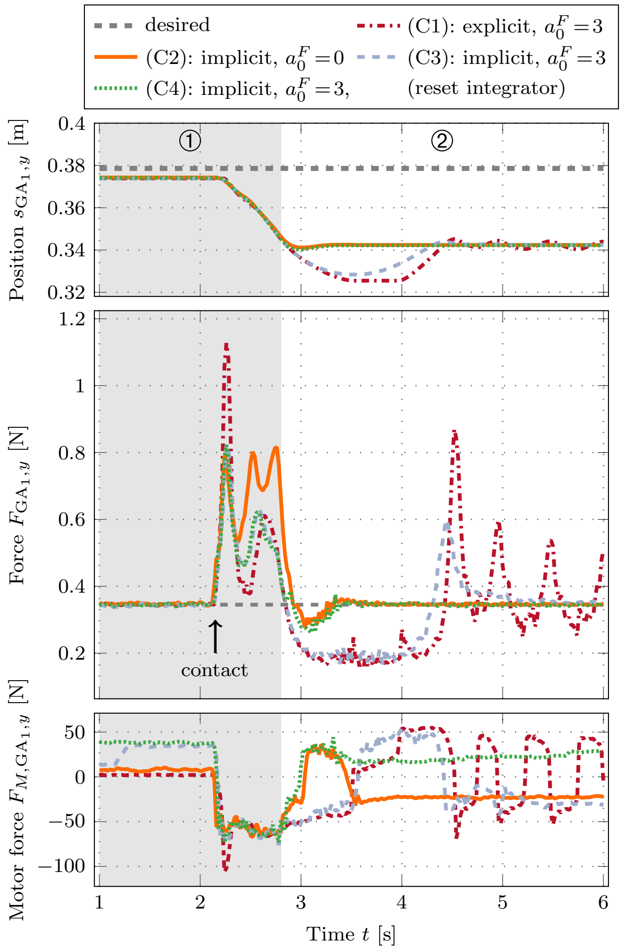

Fig. 13. Exp. 2: An external disturbance of constant velocity $v_{\mathrm{dist},z} = -100\,\mathrm{m\,s^{-1}}$ penetrates the handling material and abruptly comes to a halt in phase ②.

to the force controlled arm (GA_1), the velocity feedforward $\dot{s}^d_{\mathrm{GA}_1,y}$ requires some correction by means of the force controller. Thus, the experiment reflects a scenario, where the information that supports coordination is not perfectly known.

Fig. 12 compares measurement results of different force control strategies, see Table 4. Clearly, the performance of the explicit implementation (C1) is not satisfactory. Significant force errors occur, in particular, when the manipulator changes direction and the controller has to compensate for the friction of the ball screw drives. In contrast, the implicit implementation (C2) performs much better because the Coulomb friction is compensated by the fast inner position control loop. Fig. 12 also reveals that the additional integral term in the force error of controller (C3) does not improve the force tracking performance.

4.2 Experiment 2: Disturbance Rejection

The second experiment mimics a scenario that appears during the manufacturing of fiber reinforced plastics, i. e. the lay-up of fiber materials. While two grasping arms cooperatively handle the deformable object a disturbance caused by a consolidation tool exerts an external force on the material, see Fig. 11. The task of the force controller is to maintain the desired interaction force and thus to limit the internal material stress (potentially causing unintended fiber displacements) and prevent detaching of the material from the gripper.

To this end, both axes of the grasping arm (GA_2) and the z-axis of (GA_1) are position controlled and held at a constant set point. The force controlled y-axis of (GA_1) maintains a desired tension force of $F^d_{\mathrm{GA}_1,y} = 0.35\,\mathrm{N}$. In phase ① of the experiment, a consolidation tool penetrates the handling material at constant vertical velocity of $v_{\mathrm{dist},z} = -100\,\mathrm{m\,s^{-1}}$ which abruptly comes to a halt ($v_{\mathrm{dist},z} = 0\,\mathrm{m\,s^{-1}}$) in phase ②.

Fig. 13 provides measurement results for different force controller strategies, see Table 4. Again, the explicit implementation (C1) performs rather bad and obviously struggles with the Coulomb friction, in particular when a change of direction is required. The controller (C2) demonstrates reasonable disturbance compensation in both phases of the experiment. Nonetheless, the tension force in the penetration phase ①. This shortcoming is resolved by controller (C3) with its additional integral force error. Obviously, the integral term constrains the force error to lower values. However, once the penetration comes to a halt in phase ②, the accumulated integrator state (of phase ①) causes a

Post-print version of the article: S. Flixeder, T. Glück, and A. Kugi, "Modeling and force control for the collaborative manipulation of deformable strip-like materials", in *Proceedings of the 7th ifac symposium on mechatronic systems & 15th mechatronics forum international conference*, Loughborough, UK, Sep. 2016, pp. 95–102. DOI: 10.1016/j.ifacol.2016.10.518
The content of this post-print version is identical to the published paper but without the publisher's final layout or copy editing.

significant negative force overshoot. The force error only slowly decays due to a slow decrease of the integrator state.

To exploit the advantages of both implementations, a combination of (C2) and (C3) is introduced. The controller (C4) utilizes the integral force error from (C3) but resets the accumulated integrator state $a^F_{0,\mathrm{GA}_1,y} \int_0^t e_{F,\mathrm{GA}_1,y} \mathrm{d}\tau = 0$ for $e_{F,\mathrm{GA}_1,y} \geq 0$. According to Fig. 13, the performance of (C4) indeed combines the advantages of (C2) and (C3). Note that the controller (C4) shows similar results as (C2) and (C3) in the scenario of Section 4.1.

5. CONCLUSIONS AND OUTLOOK

This work exploits different force control strategies for the collaborative manipulation of deformable materials like textiles, leather, and foils. It is shown that the interaction stiffness plays a crucial role in the stability analysis of force control. The catenary equation serves as a simple suitable model for a variety of two side clamped materials. By considering the dynamics of the first-order low-pass force filter in the closed-loop system, necessary conditions to preserve coupled stability of the interacting manipulators are derived. The stability analysis reveals that the control performance can be considerably enhanced by a mechatronic design involving an intrinsic compliance element. The experiments on the multi-arm manipulator exposed that the explicit force control implementation is favorable over the implicit strategy. The implementations with and without force integrator exhibit specific negative aspects, whereas a purposeful combination of the two strategies proved excellent performance.

In a future work, the above results will be utilized for the coordination and on-line motion planning of multiple grasping arms and a consolidation tool. The manipulation task involves pick up, coordinated transportation, and accurate placement of strip-like deformable materials on a complex mold.

REFERENCES

Chiaverini, S., Siciliano, B., and Villani, L. (1992). A stable force/position controller for robot manipulators. In *Proc. 31st IEEE Conference on Decision and Control (CDC)*, volume 2, 1869–1874. Tucson, USA.

Colgate, J.E. and Hogan, N. (1988). Robust control of dynamically interacting systems. *International Journal of Control*, 48(1), 65–88.

De Schutter, J., Bruyninckx, H., Zhu, W.H., and Spong, M. (1998). Force control: a bird's eye view. In *Control Problems in Robotics and Automation*, volume 230 of *Lecture Notes in Control and Information Sciences*, 1–17. Springer.

Flixeder, S., Glück, T., Böck, M., and Kugi, A. (2014). Combined path following and compliance control with application to a biaxial gantry robot. In *Proc. 2014 IEEE Conference on Control Applications (CCA)*, 796–801. Antibes, France.

Grießer, M. and Taylor, P. (1996). The bending behaviour of fabrics: an energy approach. *Mathematics and Computers in Simulation*, 5(41), 579–586.

Henrich, D. and Wörn, H. (eds.) (2000). *Robot manipulation of deformable objects*. Springer.

Isidori, A. (1995). *Nonlinear Control Systems*. Springer, 3 edition.

Khalil, F.F. and Payeur, P. (2010). *Robot Manipulators Trends and Development*, chapter Dexterous robotic manipulation of deformable objects with multi-sensory feedback-a review, 587–620. InTech.

Koustoumpardis, P.N. and Aspragathos, N.A. (2008). Robot-human cooperation holding and handling a piece of fabric. In *Proc. 11th International Conference on Climbing and Walking Robots and Support Technologies for Mobile Machines (CLAWAR)*, 820–827. Coimbra, Portugal.

Koustoumpardis, P.N., Chatzilygeroudis, K.I., Synodinos, A.I., and Aspragathos, N.A. (2016). Human robot collaboration for folding fabrics based on force/rgb-d feedback. In *Proc. 24th International Conference on Robotics in Alpe-Adria-Danube Region (RAAD)*, 235–243. RAAD, Bucharest, Romania.

Krebs, F., Larsen, L., Braun, G., and Dudenhausen, W. (2013). Design of a multifunctional cell for aerospace cfrp production. In *Proc. 23rd International Conference on Flexible Automation & Intelligent Manufacturing*, 515–524. Porto, Portugal.

Kruse, D., Radke, R., and Wen, J. (2015). Collaborative human-robot manipulation of highly deformable materials. In *Proc. 2015 IEEE Conference on Robotics and Automation (ICRA)*, 3782–3787. Seattle, USA.

Lankalapalli, S. and Eischen, J.W. (2003). Optimal pick-up locations for transport and handling of limp materials part i: One-dimensional strips. *Textile research journal*, 73(9), 787–796.

Routh, E. (1891). *A Treatise on Analytical Statics: On strings*. 1. Cambridge University Press.

Saadat, M. and Nan, P. (2002). Industrial applications of automatic manipulation of flexible materials. *Industrial Robot: An International Journal*, 29(5), 434 – 442.

Šurdilović, D. (2007). Robust control design of impedance control for industrial robots. In *Proc. 2007 IEEE/RSJ International Conference on Intelligent Robots and Systems (IROS)*, 3572–3579. San Diego, USA.

Šurdilović, D., Yakut, Y., Nguyen, T.M., Pham, X.B., Vick, A., and Martin-Martin, R. (2010). Compliance control with dual-arm humanoid robots: Design, planning and programming. In *Proc. 10th IEEE-RAS International Conference on Humanoid Robots (Humanoids)*, 275–281. Nashville, USA.

Syerko, E., Comas-Cardona, S., and Binetruy, C. (2012). Models of mechanical properties/behavior of dry fibrous materials at various scales in bending and tension: A review. *Composites Part A: Applied Science and Manufacturing*, 43(8), 1365–1388.

Vukobratovic, M., Šurdilović, D., Ekalo, Y., and Katic, D. (2009). *Dynamics and robust control of robot-environment interaction*, volume 2 of *New frontiers in robotics*. World Scientific.

Wedel, D. and Saridis, G. (1988). An experiment in hybrid position/force control of a six dof revolute manipulator. In *Proc. 1988 IEEE International Conference on Robotics and Automation*, volume 3, 1638–1642. Philadelphia, USA.

Zeng, G. and Hemami, A. (1997). An overview of robot force control. *Robotica*, 15(5), 473–482.

Post-print version of the article: S. Flixeder, T. Glück, and A. Kugi, "Modeling and force control for the collaborative manipulation of deformable strip-like materials", in *Proceedings of the 7th ifac symposium on mechatronic systems & 15th mechatronics forum international conference*, Loughborough, UK, Sep. 2016, pp. 95–102. DOI: 10.1016/j.ifacol.2016.10.518